EGTRIB Journal
JOURNAL OF
THE EGYPTIAN SOCIETY OF TRIBOLOGY
VOLUME 17, No. 2, April 2020, pp. 23 - 39 **ISSN 2090 - 5882**
(Received December 28. 2019, Accepted in final form February 27. 2020) **www.egtribjournal.com**

DETECTION OF LOCALIZED FAULT IN INNER RACE OF DEEP GROOVE BALL BEARING BASED ON MSC-ADAMS

Nabhan A.*, Rashed A.

Faculty of Engineering, Minia University, El-Minia 61111, EGYPT.
Corresponding author E-mail: *a.nabhan@minia.edu.eg

ABSTRACT
This work aims to enhance an approach to detect localized fault on the inner race of deep groove ball bearing in presence of generated vibration. Experiments is equipped to measure vibrations signals for different sizes of deep groove ball bearing in the presence of localized surface fault to diagnosis the unhealthy bearing. Dynamic model based on MSC-ADAMS can serve as a tool to obtain vibration responses that generated due to the bearing faults. Root mean square (RMS), crest factor, kurtosis and skewness will serve as indicators of average amplitude of envelope analysis signals. The vibration signals pattern collected from the simulation model and experimental data have the same results. The accelerometers attach in two positions to determine the suitable detection method of a fault on the inner race on both the loaded and un-loaded zones. It can be concluded that the acceleration RMS ratio is more effective in detecting the defect for acceleration response. Also the acceleration kurtosis ratios may be used to detect the fault located at the loaded zone. While acceleration crest factor and skewness ratios are failed to indicate the fault diagnosis.

KEYWORDS
Simulation Model, Inner race fault, ADAMS and statistical parameter.

INTRODUCTION
Among the mechanical components, researchers pay great attention to the rolling element bearings due to their unquestionable industrial importance. In order to study the behavior of vibration analysis for monitoring bearing health condition in practice, a test rigs had been built. The main purpose of building the test rig was to provide vibrational data under controlled operating conditions of applied load and rotational speed. Several different damage processes introduced on a number of bearings and each tested under different loads and speeds. There are many studies on the dynamic behavior of bearings based on the analysis of experimental signals. Some of them look for defects located in the outer race with statistical methods such as Fast Fourier Transform [1–3] or exact methods of frequency and wavelet analysis [4], and using these parameters to feed a vibration profiles describing the condition, [5, 6]. A theoretical model for the effect function created on the structure, where a rolling element negotiates a spall-like defect in the internal race, which

is considered a moving race. The negotiation of imbalance was a series of events for the purpose of understanding the physics behind this negotiation, [7]. A method has been proposed for modeling a non-ideal rolling ball joint with local defects in multi-body systems. The kinetic constraints of the ideal revolutionary articulation are released in the theory of traditional multi-body dynamics, and the functions of the non-ideal carrier articulation Built using interactions due to contact forces. Local defects of a certain arc length and depth are created for the track surface, [8]. An approach based on the principles of engineering mechanics is used to obtain a time function of impact force which is then used to simulate the response of the bearing housing. This response is analyzed in the time and frequency domains to get an idea of the load error and its size. Experiments conducted with deep groove ball bearings with different defect sizes and speeds show an acceptable relationship with theoretical simulation. Thus, the impact-based model has developed a theoretical platform to gain insight into physical phenomena, which are not measured in practice, through the mechanism of triggering the effect and can withstand enough potential to withstand fault identification, [9]. Determination of the effect of the external race defect of deep groove ball bearings through experimental and numerical methods. Three-dimensional finite element model of housing and exterior race was simulated using the commercial package ABAQUS/CAE, [10]. Moreover, the effect of the number of external race defects in deep groove balls is examined using experimental and numerical methods. A three-dimensional model of housing and external race was developed using ABAQUS, [11]. The vibration signal decomposition using discrete wavelet transformation with the help of sym5 wavelet were displayed. Symlet wavelet is characterized by the linear nature of the phase which keeps the signal sharp even when a sudden change in signal occurs, [12]. The decaying signal is divided into the peak corresponding to the entry and exit of the ball, which allows to estimate the size of the defect in the bearing. The dynamic behaviors of a single EHL between a rolling element and raceways under load and speed ranges are numerically analyzed based on the transient EHL model and the free vibration model, [13]. The discrete convolution and fast Fourier transform method is applied to increase the computational efficiency associated with elastic deformations and a semi-system approach is applied to improve solution convergence in extreme conditions. A dynamic model of ball bearings is established with ADAMS, [14]. Three types of fault signal vibration response were obtained from different sizes of the outer ring bearing. According to the bearing interval failure tolerance double fault response can achieve quantitative analysis of bearing fault. Three different models with increased level of familiarity are considered, [15]. A schematic model of the MATLAB Simulink-based kinetic motion mass which does not explicitly consider the dynamics of the cage and traction, and a detailed multi-body spatial dynamic model with complex contact and traction mechanics developed using ADAMS software. The study shows the dynamic motion of a ball bearing cage immersed in a cooled liquid under high-speed conditions, [16]. The dynamic motion of the cage was studied as a function in the clearance of the ball- cage pocket and ball cage of different internal rotation speeds under light load conditions. However, the probability density function curves indicate that the increase in rotor speed increases the standard deviation in the cage rotation frequency. The loss of corrosion in the cage was greater for the largest land-cage and less clearance of the ball cage pocket. A dynamic model of ball bearings with a localized defect in the outer raceways to analyze the effect of contrast variation on the vibration response of damaged bearings, Numerical analysis and experimental results show that grease with a

different level of viscosity affects the defective bearing's vibration signal, [17]. The nonlinear dynamic behaviors of the rolling bearing specifically, a new dynamic model of the rolling bearing was created based on the LaGrange approach, [18]. A method to determine the severity of the cage fault in the bearing with the help of a dynamic model based on the contact mechanics applied to the case of external harmonic excitation, [19]. In addition, the study of air gap difference to predict the frequency of faults and loss of stiffness in the rolling element bearings. A new approach is used to calculate the contact force in the ball-raceway in the fault zone based on the pressure distribution and the contact area, [20]. The relative motion between the inner ring, the outer ring, and the balls is considered in the proposed model, and the Runge-Kutta algorithm is used to solve the vibration equations. In addition, vibration experiments of the bearing with defect in the outer ring are carried out under different loads. The additional deviation of the rolling elements in the presence of a local defect was studied while simulating the defect in the dynamic model, [21]. The equations derived from the motions were solved analytically using the fourth order Runge-Kutta method in MATLAB. The vibrations resulting from dry and lubricated contact bearings that have local defects on their races have been theoretically and experimentally studied. Vibration generation was studied by point defect in the rolling element loader as a function of bearing rotation, load distribution in the bearing, elasticity of bearing structure, oil film properties, and the transport path between the bearing and the power adapter, [22]. A new application has been developed to simulate the response of vibratory bearings to the excitement caused by localized defects.

Based on the papers results that displayed on the previous literature review, the main objective of the research is to create a dynamic model that simulates deep groove bearing with localized fault on the inner race. The dynamic model of defected bearing is established using MSC-ADAMS. The vibration analysis are collected using acceleration signals that examined with the statistical parameters, RMS - crest factor - kurtosis - skewness, to determine the appropriate method to detect the diagnosis of the defect.

Geometry of a Ball Bearing

The study is based on the use of the single-row, deep-groove ball bearing, SKF 6004. The geometrical parameters of the bearing are

Table 1. Geometrical parameters of the bearing.

Outer diameter, D_o	**42 mm**
Bore diameter, d	**20 mm**
Pitch diameter, d_p	**31 mm**
Raceway width, B	**12 mm**
Ball diameter, d_b	**6.35 mm**
Contact angle, α	**0°**
Number of Balls, n_b	**9**

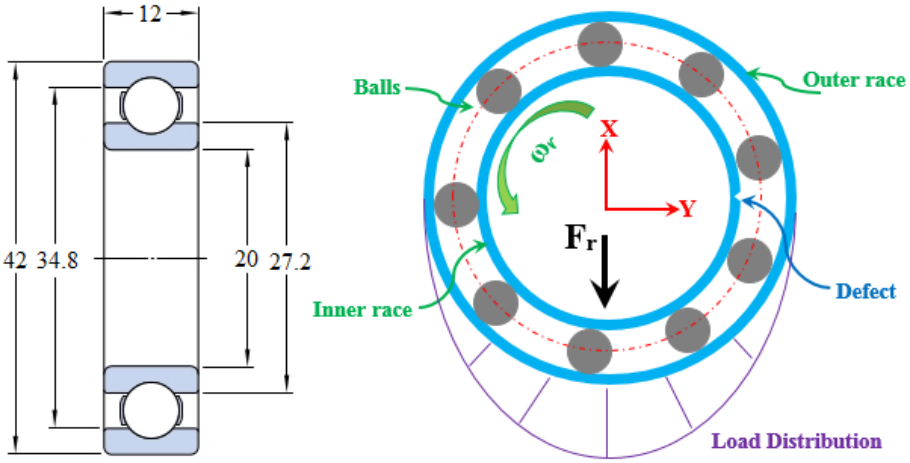

Fig. 1 Geometry of the deep groove ball bearing SKF 6004.

EXPERIMENTS

The experimental stand consists of a three-phase motor with rotary encoder fitted on the second shaft end. The motor is actuated with the control unit with a frequency converter for continuous adjustment of the speed. An elastic claw coupling is utilized to dampen the oscillation generated by the motor. The shaft is supported by two ball bearings, one is healthy and the other is defective inner race. The piezo-electric acceleration sensor (IMI sensors 603C01) are fitted to collect the vibration signal data of the defected bearing in both vertical and horizontal directions. Moreover, the reference transducer (OZDK 10P5101/S35A) is used to record the rotational speed. The acceleration sensor and reference transducer are connected to the measuring amplifier. The measuring amplifier, with gain factor1, 10, or 100, supplies the acceleration sensors with current and boosts the signals from the acceleration signals. The signal is then digitized a data acquisition card (BMC USB-AD16F) and transferred to the PC, where the recording of the experiments was carried out using the LabVIEW interface. Figure 1 illustrates a schematic of test setup including the measurement equipment.

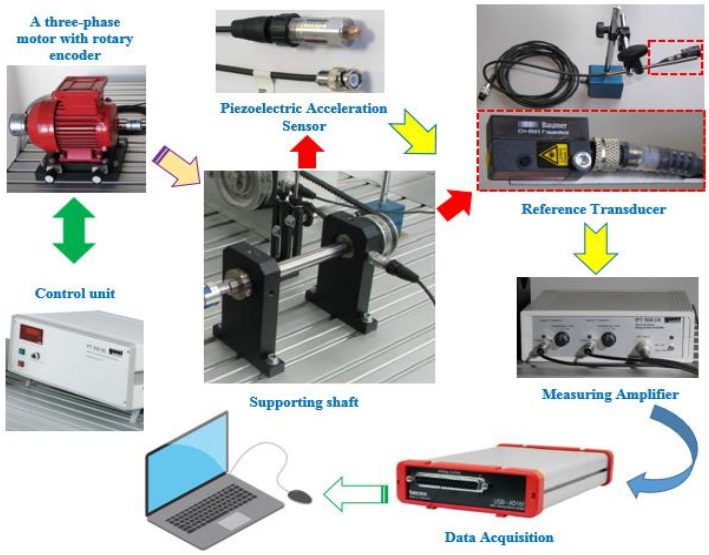

Fig. 2 A schematic of the experimental Stand including the measurement equipment.

Bearing System Model

To analyze the structural vibrations affecting rolling element bearings, a number of assumptions are made here. The contact stress and deformation between balls and the bearing races governed by the Hertzian contact theory of elasticity. A non-linear relationship for load deformation can be used to compute deformation, [1].

$$Q = K\delta^{n} \quad (1)$$

The value of load–deflection exponent "n" = 1.5 for ball bearings, and the load-deflection factor "K" depends on the contact between ball and race. The equivalent load deflection factor between the inner and outer races can be estimated as the sum of the contact stiffness between balls and each race.

$$K = \left(\frac{1}{(1/K_{in})^{1/n} + (1/K_{out})^{1/n}}\right)^{n} \quad (2)$$

The relationship between ball-inner race contact stiffness, K_{in}, and ball-outer race contact stiffness, K_{out}, is given by.

$$K_{in}/K_{out} = 2.15 * 10^{5} * \sum [\rho_{in}/\rho_{out}]^{-1/2} * \left(\delta^{*}_{in/out}\right)^{-3/2} \quad (3)$$

For a rigidly supported bearing subjected to a radial load, the radial deflection of i^{th} ball at any angle φ_i is given by

$$\delta_r = \delta_{max}\left[1 - \frac{1}{2\,\varepsilon}(1 - \cos\varphi_i)\right] \quad (4)$$

$$\varepsilon = \frac{1}{2}\left(1 - \frac{P_d}{2\,\delta_r}\right) \quad (5)$$

Where, P_d is the diametric clearance, ε is the load distribution factor.

The position of any rolling element, φ_i, at any time, t, with respect to its initial position, φ_o, depends on angular velocity of cage, ω_c, and number of rolling elements, n_b, in bearings

$$\varphi_i = \frac{2\pi i}{n_b} + \omega_c t + \varphi_o \quad (6)$$

Fundamental cage angular velocity

$$\omega_c = \frac{\omega_s}{2}\left(1 - \frac{d_b}{d_p}\cos\alpha\right) \quad (7)$$

The angular extent of the load distribution zone is determined using the following equation

$$\varphi_l = \cos^{-1} P_d/2\delta_r \quad (8)$$

For ball bearings having zero clearance zero clearance, ε = 0.5, a radial load intensity around the race circumference, under external radial load F_r, can be determined using

$$Q_\varphi = Q_{max}[1 - \frac{1}{2\,\varepsilon}(1 - \cos\varphi)]^{n} \quad (9)$$

$$Q_{max} = \frac{4.37\,F_r}{n_b \cos\alpha} \quad (10)$$

The high frequency structural vibrations detected on the rolling element bearing system is due to the external radial force. In this simplified bearing system model, as illustrates in Figure 3, the outer race is stationary and the inner race is pressed onto the rotating shaft and thus rotates with it. The load path is from the shaft, to the inner race, to the balls, to the outer race, and finally to the housing. The outer bearing race is considered to be perfectly circular and rigidly fixed and no relative motion is permitted on the contact surface. All balls are presumed to be perfectly spherical and of equal diameter. In Figure

3, M_S, K_S and C_S are equivalent rotor shaft mass, stiffness and damping, respectively. K_i, C_i and M_i are stiffness, damping and mass of the inner race. K_b, C_b and M_b are stiffness, damping and mass of the roller element (ball). K_o, C_o and M_o are stiffness, damping and mass of the outer race. While, K_{sm}, C_{sm} and M_{sm} are stiffness, damping and mass of the sprung mass system.

The contact deformation can be computed by following relation

$$\delta_i = (x_d \cos\varphi_i + y_d \cos\varphi_i - c_r) \quad (11)$$

Where, x_d and y_d are the relative displacement between inner race and ball for inner race fault and outer race and ball for outer race fault in x and y directions, respectively and the internal radial clearance, C_r, can be computed using equation

$$C_r = \frac{P_d}{2 * (1 - \cos\varphi)} \quad (12)$$

A non-linear relationship for load deformation in horizontal (Q_x) and vertical (Q_y) directions, governed by the Hertzian contact theory of elasticity, are written as

$$Q_x = \sum_{i=1}^{n_b} K \delta_i^n \cos\varphi_i \,.\, h(-\delta_i) \quad (13)$$

$$Q_y = \sum_{i=1}^{n_b} K \delta_i^n \sin\varphi_i \,.\, h(-\delta_i) \quad (14)$$

The Heaviside function is given by

$$h(x) = \begin{cases} 1 & \text{for } x \geq 0 \\ 0 & \text{for } x \leq 0 \end{cases} \quad (15)$$

Table 1. Parameters of the ball bearing model.

Mass of ball, M_b	**1.05 g**
Stiffness of ball, K_b	**$1.62 * 10^{10}$ N/m**
Damping of ball, C_b	**1350 Ns/m**
Mass of inner race, M_i	**20.27g**
Stiffness of inner race, K_i	**$15.1*10^6$ N/m**
Damping of inner race, C_i	**2000 Ns/m**
Mass of outer race, M_o	**29.36 g**
Stiffness of outer race, K_o	**$15 *10^6$ N/m**
Damping of outer race, C_o	**2000 Ns/m**
Mass of outer race, M_{sm}	**500 g**
Stiffness of outer race, K_{sm}	**$8.9*10^7$ N/m**
Damping of outer race, C_{sm}	**1250 Ns/m**

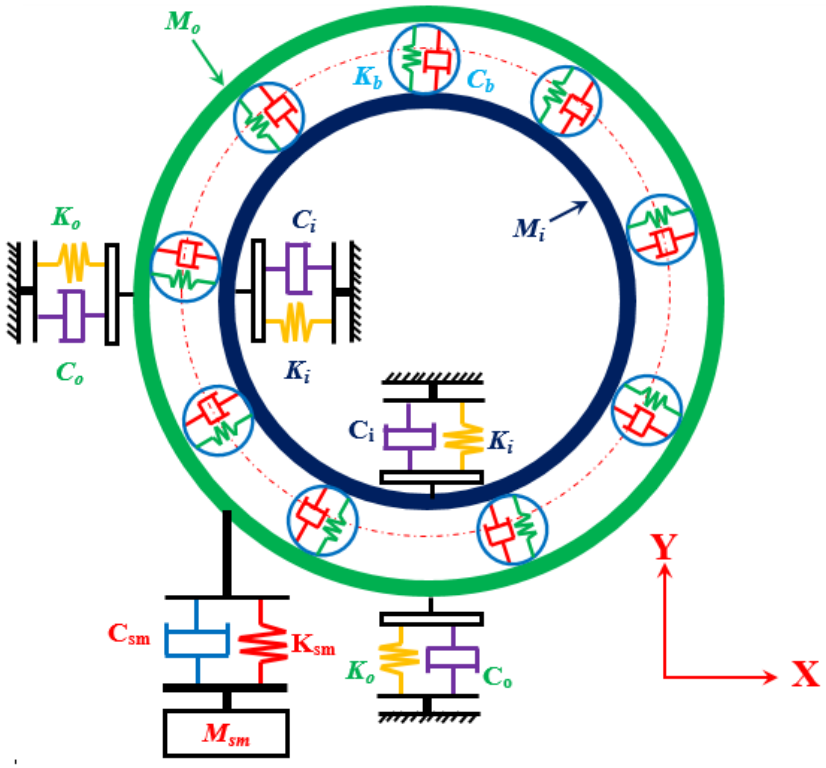

Fig. 3 Free body diagram of shaft-bearing system.

According to the bearing model in Figure 3, the bearing outer and inner races is modelled as a two degrees of freedom system. The general governing equations can be expressed as
The outer race equations

$$M_o\ddot{x}_o = F_x + C_o\dot{x}_o + k_o x_o \quad (16)$$

$$M_o\ddot{y}_o = F_y - M_o g - (C_o + C_{sm})\dot{y}_o - (k_o + K_{sm})y_o + k_{sm}y_{sm} + C_{sm}\dot{y}_{sm} \quad (17)$$

Where x_o and y_o are x and y displacements of outer race center of mass (also geometric center), y_{sm} is displacement of sprung mass, and g is acceleration due to gravity.
The inner race equations

$$M_i\ddot{x}_i = -F_x + C_i\dot{x}_i + k_i x_i \quad (18)$$

$$M_i\ddot{y}_i = -F_y - M_i g - C_i\dot{y}_i - k_i x_i \quad (19)$$

The ball equation

$$M_b\ddot{x}_b = -C_b\dot{x}_b - k_b x_b \quad (20)$$

Where, $x_b = (x_o - x_i)$
The sprung mass is attached in y direction. Its equation of motion can be written as

$$M_{sm}\ddot{y}_{sm} = -M_{sm}g + C_{sm}(\dot{y}_o + \dot{y}_{sm}) + K_{sm}(y_o + y_{sm}) \quad (21)$$

Modelling localized inner race fault
The existence of one of the fault frequencies in the direct or processed frequency spectrum is the powerful sign of the fault. The characteristic inner race defect frequency is given for a bearing with stationary outer ring by the following formulae;

$$\omega_i = \frac{n_p\omega_s}{2}\left(1 + \frac{d_b}{d_p}\cos\alpha\right) \quad (22)$$

The model is equipped with a small rectangular spall in the inner race as shown in Figure 4. A spall dimensions are, (t) as a fault width and (h) as a fault depth. $\Delta\varphi_d$ is a specific angular position at which the balls' track marks the defect area on the inner race.

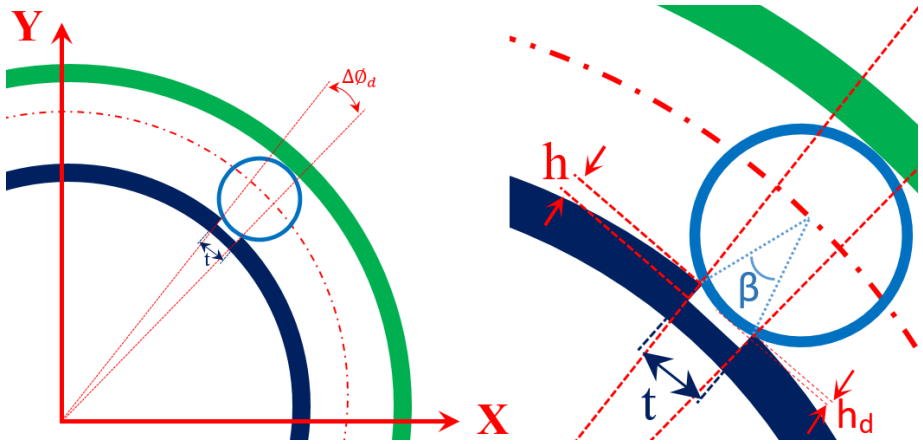

Fig. 4 Ball-inner race fault contact.

As a result of the rotation of the inner race, the location of the fault is constantly changing which makes φ_d value is dependent on the shaft angular velocity which can be expressed as

$$\Delta\varphi_d = \omega_s t + \varphi_0 \quad (23)$$

Where, φ_0 is the initial location of spall. The contact deformation for bearing with inner race fault is given as

$$\delta_i = (x_d \cos\varphi_i + y_d \cos\varphi_i - C_r - \delta_f) \quad (24)$$

The contact deformation for the fault is depending on the fault width and the ball diameter which can be expressed as

$$\delta_f = \begin{cases} h_d & \text{if } \varphi_d \le \varphi_i \le \Delta\varphi_d \\ 0 & \text{otherwise} \end{cases} \quad (25)$$

The depth value of falling ball inside the fault can be calculated

$$h_d = \frac{d_p}{2}\left(1 - \sqrt{1 - (t/d_p)^2}\right) \quad (26)$$

Ball Bearing Model by MSC-ADAMS

ADAMS is commercially available virtual prototyping software, which allows the user to model a mechanical system, and mathematically simulate and visualize its 3D motion and force behavior under real-world operating conditions. MSC-ADAMS automatically converts a graphically defined model to dynamic equations of motion, and then solves the equations, typically in the time domain. The deep groove ball bearing works on the principle of decrease friction force to minimum value. The modeling process begins with drawn the present deep groove ball bearing (6004) then after selecting units' system, gravity setting, and coordinate systems. The fixed parts and ground reference frame were defined to determine the global coordinate system. The model of the ball bearing mechanism shown in Figure 5. The second step defined the measures for the model, acceleration verses time. The stiffness parameters values are defined similarly to frequency response that found from the experiment data. In the present analysis, a model of fault bearing with localized faults on inner race is established as small notches of rectangular shape. Figure 6 illustrates the flow chart of simulation run. The fault is

established as rectangular spall in the inner race with dimensions of (0.25 - 0.50 – 0.75) mm as a fault width and (0.5 - 1.0 – 1.5) mm as a fault depth.

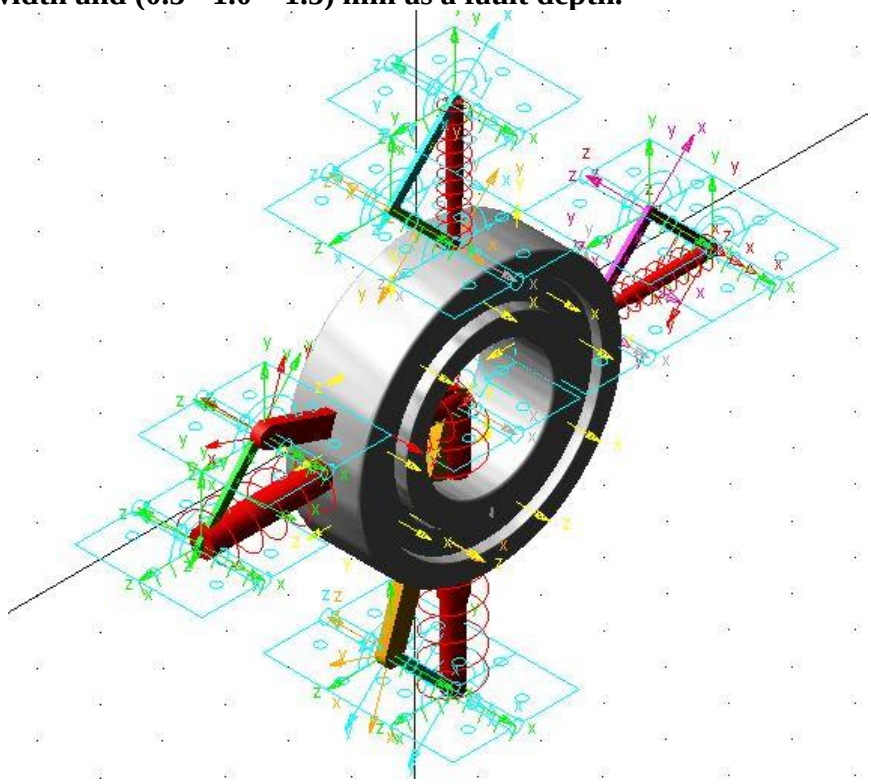

Fig. 5 Model of deep groove ball bearing in MSC-ADAMS.

Experimental and Simulation Data Validation

The collected acceleration signals from the experiments were compared with that from MSC-ADAMS model to check of the accordance of the model. The simulation data were exported to MATLAB for processing because of ADAMS does not always output time and frequency charts data. Figures 7 and 8 illustrate the typical waveform of the healthy bearing in time and frequency domain analysis techniques for the experimental and simulation data, respectively. The vibration data are carried out under a shaft rotational speed of 1500 rpm (25 Hz). It can observed that, the time domain signals displays a clear regular waveform with small peak less than 0.7 m/sec^2 in acceleration amplitude. In the envelope spectrum analysis, the largest amplitude is at the shaft running speed of 25 Hz. Therefore, the spectrum of a healthy bearing displays no frequencies other than shaft rotational frequency.

Bearing with inner race defect manifests in a similar way as defect of outer race but the difference is the inner race defect is located in relative movement to the load zone. The movement of the defect leads to amplitude modulated impact excitation. The time domain displays an irregular waveform that has a high peak approximately 20 m/sec^2 in acceleration amplitude, as shown in Figure 9. Therefore, in the frequency spectrum, in addition to the peak for the inner race defect and the peak rotational frequency, side bands to the inner race defect can be identified at a distance of the rotational frequency of the inner race. The effects of circular damage undergo amplitude attenuation. Experimental as well as simulated data in Figure 10 shows, shaft speed "ω_s" of 25 Hz and

the defect frequency (fundamental frequency) of the inner race "ω_i" is located at 135 Hz. The side bands of the defect frequency can be seen at a distance of the speed +/- ω_s. The side bands is repeated for the harmonics. Thus, ADAMS model gives a result that is nearly similar with the experimental results.

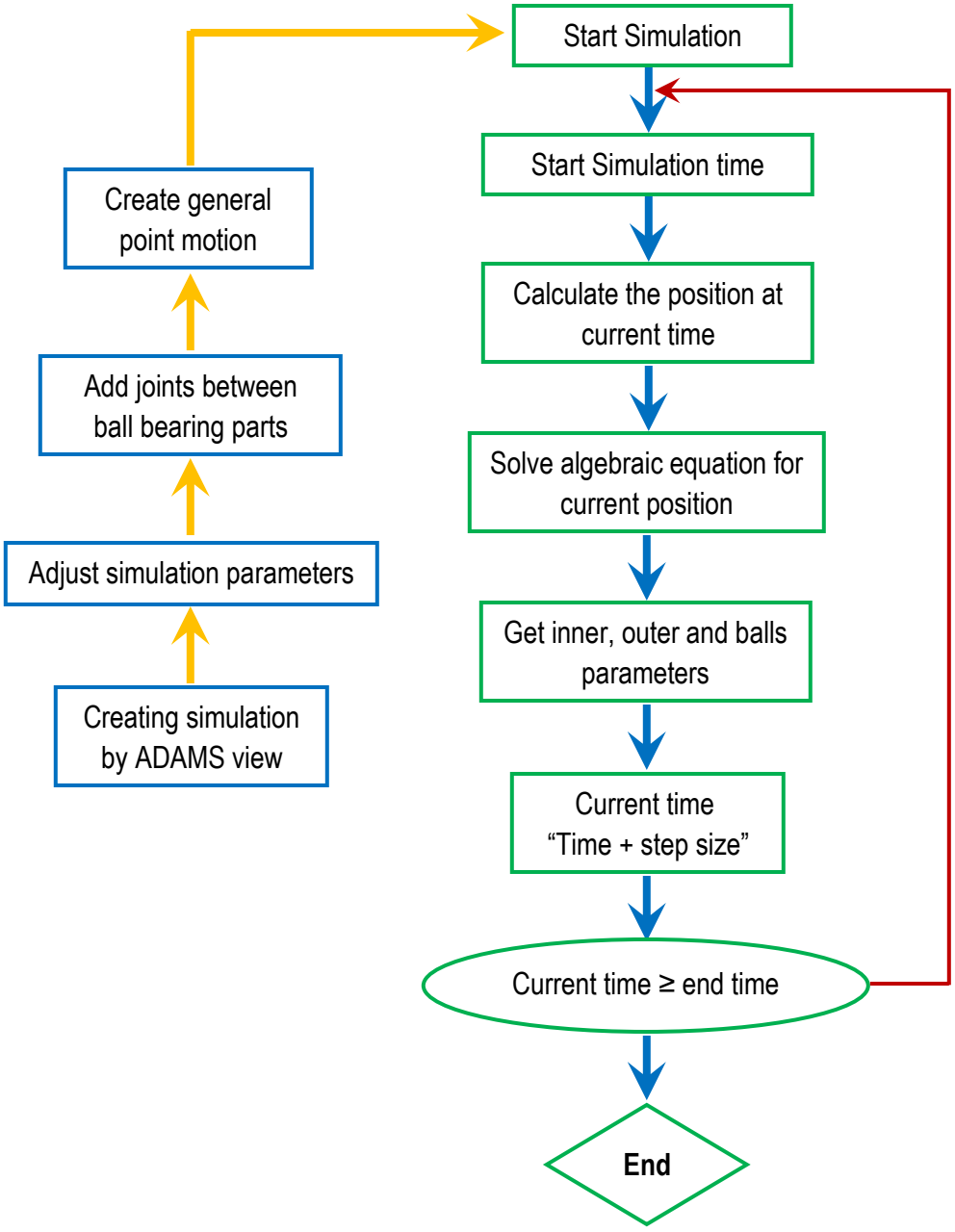

Fig. 6 Simulation flow chart run.

Inner Race Fault Detection

The fault detection mechanism located in inner race is related to an impulse occurs when a rolling elements passes and strikes the fault position. The statistical parameters for the acceleration responses have been used as one-off and trend parameters in an attempt to detect the presence of incipient bearing damage, given in Figures 11-12. The vibration

data are calculated for accelerometer positions, loaded and unloaded zone, for a broad range of rotational speed ranging from 500 to 3000 rpm. The ratio the statistical parameters between the acceleration responses of the fault inner race bearing to that of the healthy one.

It can observed from Figure 11a that the acceleration RMS ratios can be effectively used to detect a fault on the inner race for all faults size for the sensor attached in the loaded zone, almost at every rotational speed. The acceleration RMS ratios increase with increasing rotational speeds as shown in Figure 11a. Where Figure 11b shows that the acceleration crest factor ratios may fail to detect the fault. It can be noticed that the acceleration kurtosis ratios may be used but the kurtosis ratios is likely to use less benefit than RMS ratios because of the resulting values in this case are less, as illustrated in Figure 11c. The same situation is valid for the acceleration RMS, crest factor and kurtosis ratios for un-loaded zone shown in Figure 12a, b and c respectively. Furthermore, the acceleration skewness ratios are failed to indicate the fault diagnosis for the sensor attached in the loaded zone, in contrast it may be used only for un-loaded zone as shown in Figures 11d and 12d. It can be concluded that, the acceleration RMS ratios are good indicator for inner race fault detection. The results showed a concordance with previous studies into for inner race fault detection, [6].

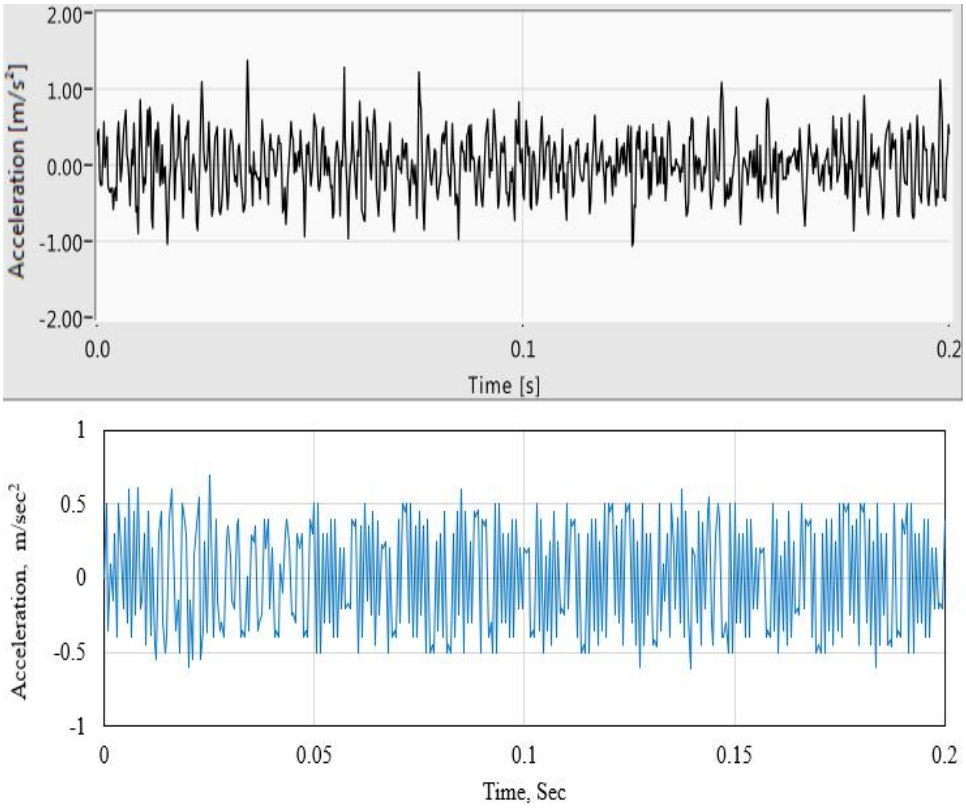

Fig. 7 Time domain signals of healthy bearing from experimental and modeling.

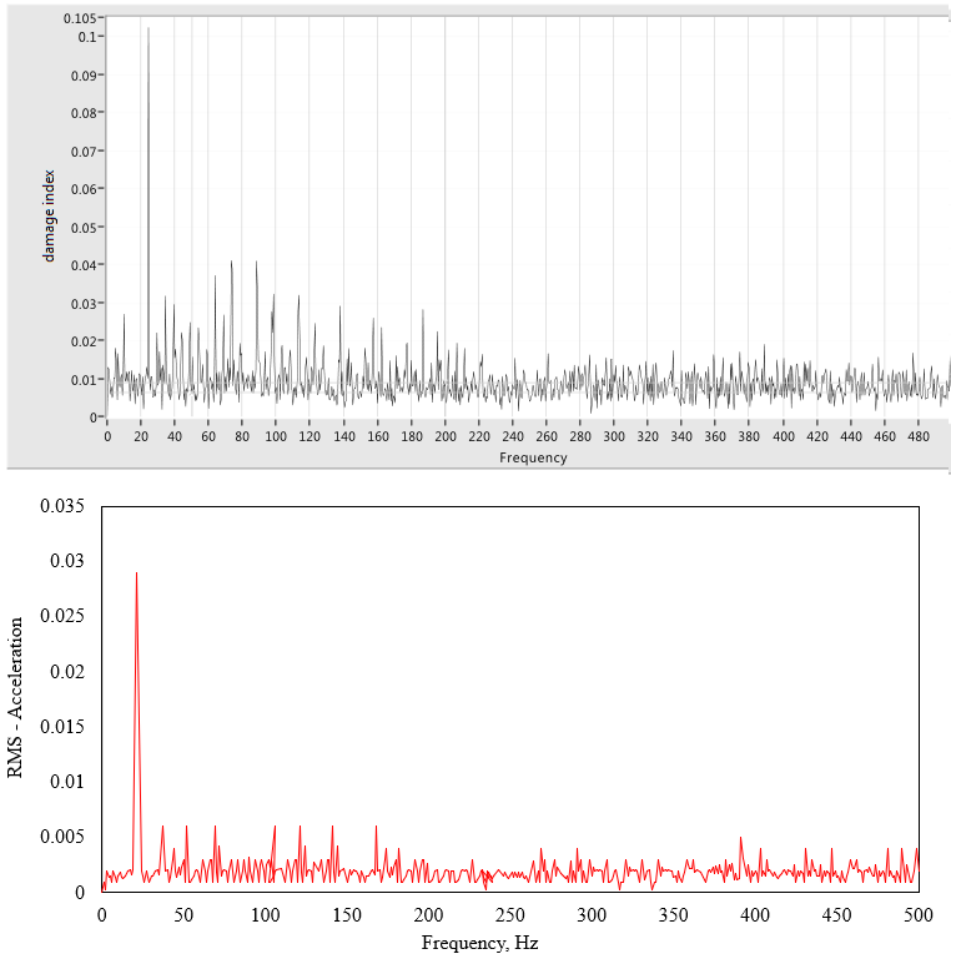

Fig. 8 Frequency domain signals of healthy bearing from experimental and modeling.

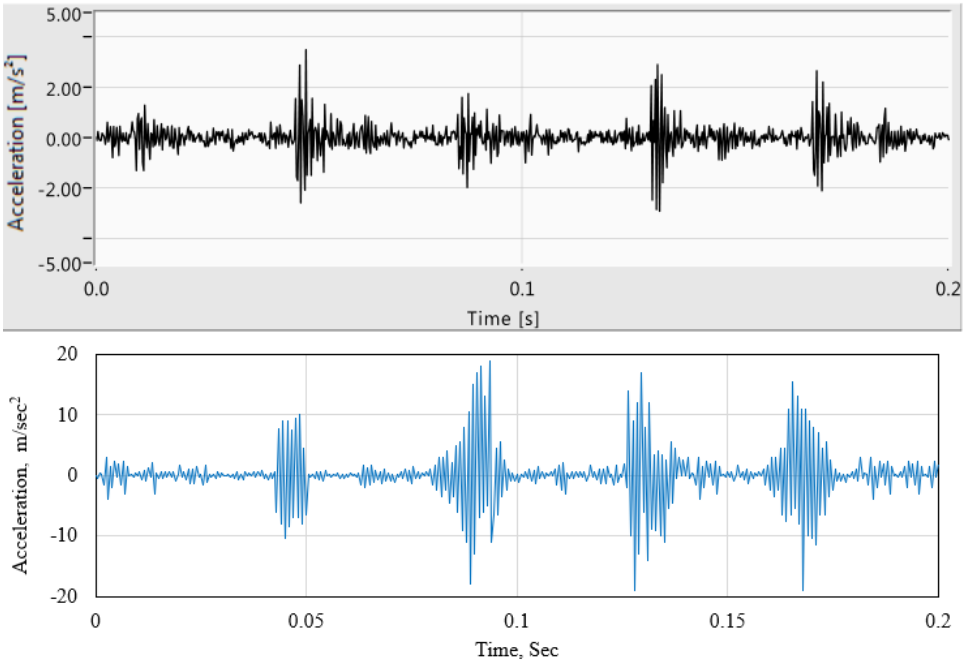

Fig. 9. Time domain signals of Defected bearing from experimental and modeling.

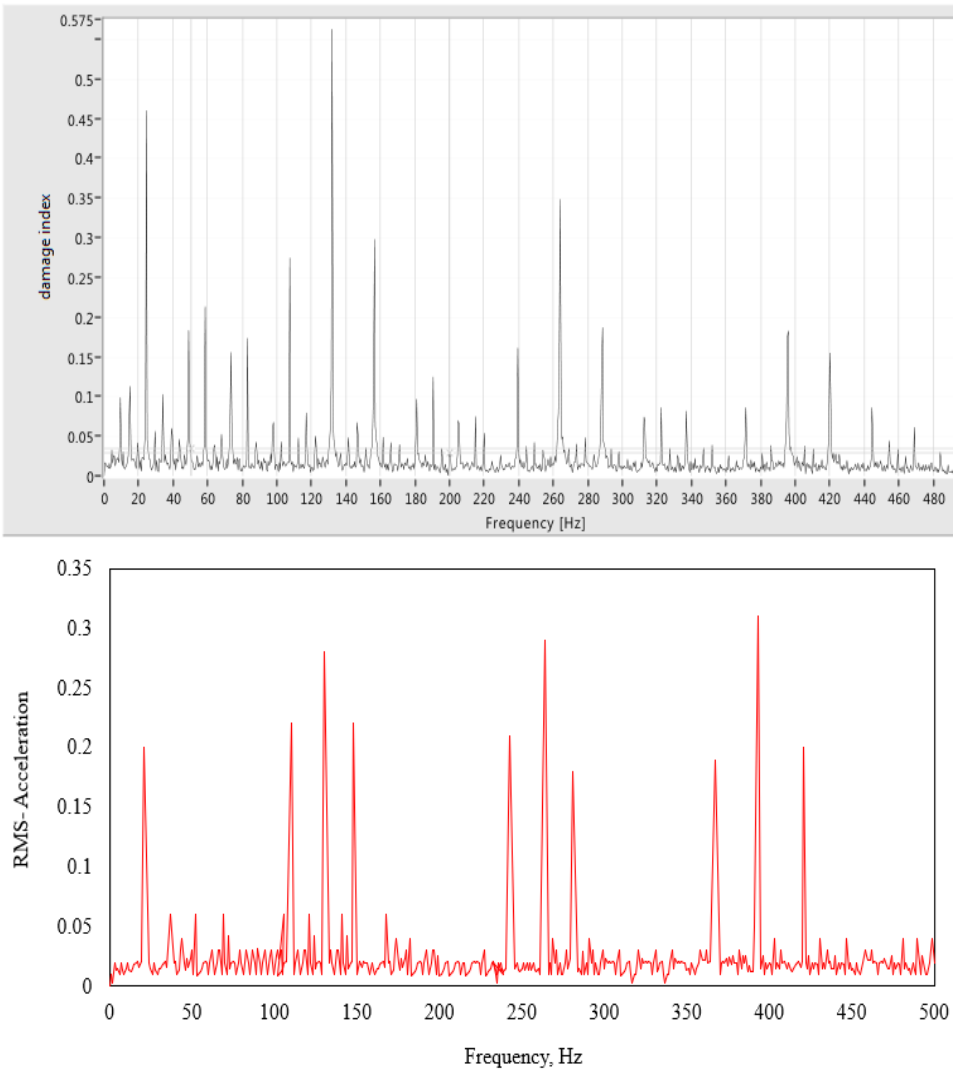

Fig. 10 Frequency domain signals of Defected bearing from experimental and modeling.

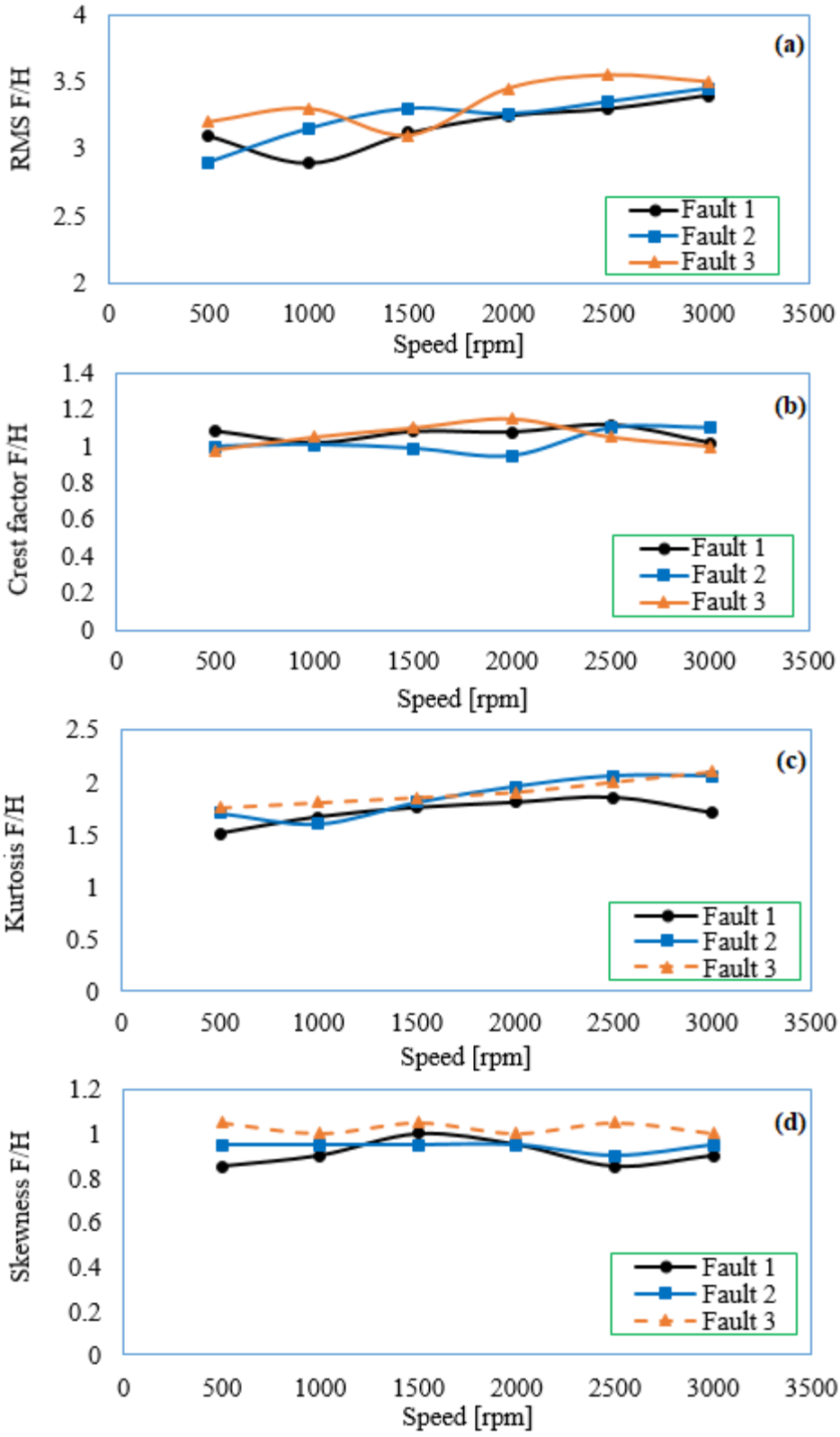

Fig. 11 Acceleration response of inner race fault at loaded zone (a) RMS (b) Crest factor, (c) kurtosis and (d) skewness.

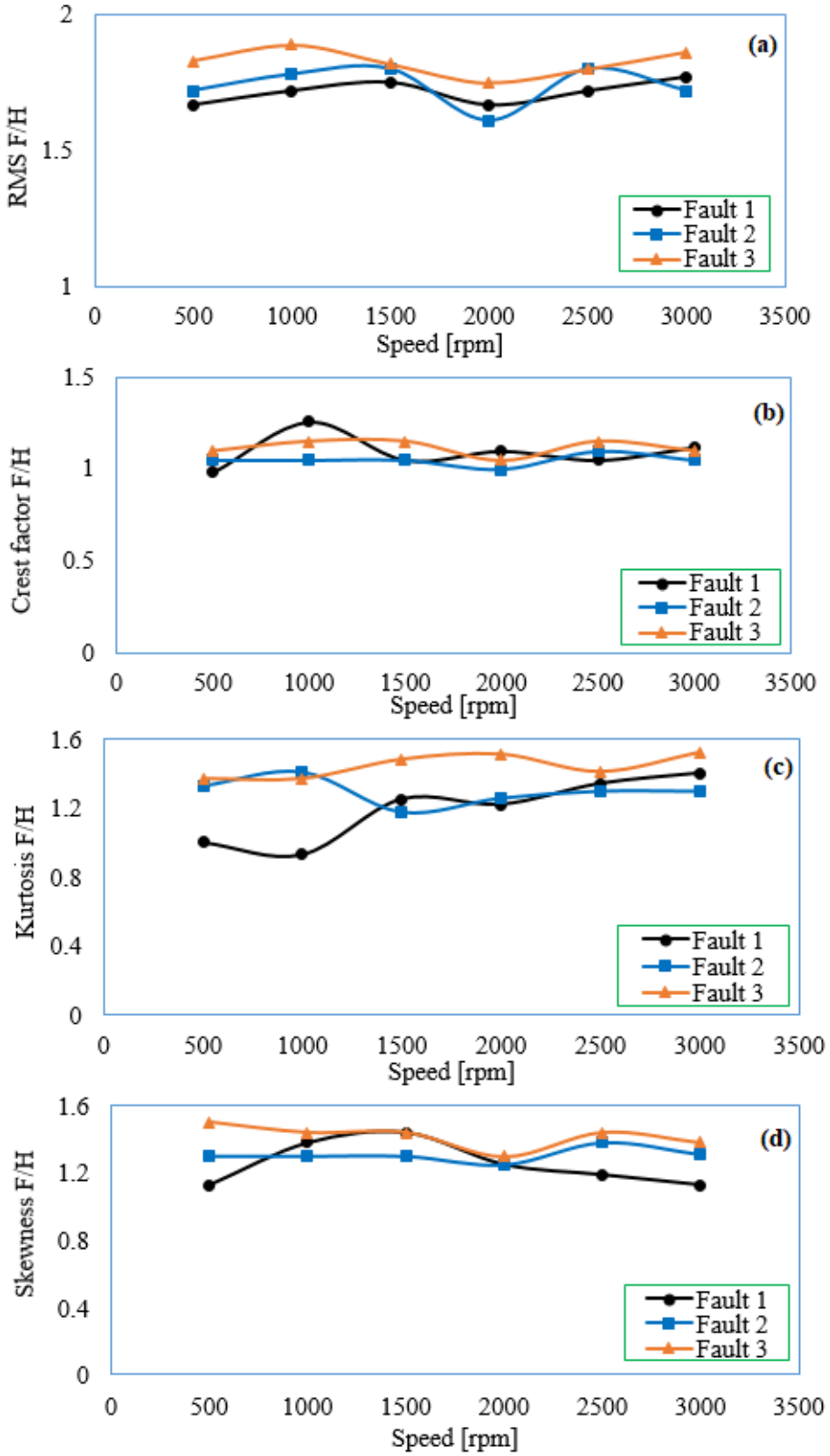

Fig. 12 Acceleration response of inner race fault at un-loaded zone (a) RMS (b) Crest factor, (c) kurtosis and (d) skewness.

CONCLUSIONS

Based on the results from the dynamic model, MSC-ADAMS model is developed and validated experimental results. Numerical model is able to predict the dynamic characteristics of the faulted inner race bearing. In addition, the results of the analysis show that the acceleration RMS ratios are appropriate parameters to collect the vibration signatures for any installed accelerometer positions. While the crest factor ratios for acceleration responses are not suitable indicator for defect detection. The results also show that the acceleration kurtosis ratios may be a good indicator for inner race fault detection. The acceleration skewness ratios are weak indicators for fault detection for sensor location at loaded zone. Furthermore, the acceleration skewness ratios for unloaded position seems to be a suitable sensor location to detect the inner race faults.

ACKNOWLEDGMENT

The authors wish to express their deep and sincere gratitude to our families for their continuous and unparalleled love, help and support.

REFERENCES

1. **Liu J., Shao Y., Lim T. C., "Vibration analysis of ball bearings with a localized defect applying piecewise response function", Mechanism and Machine Theory, Vol. 56, pp. 156–169, (2012).**
2. **Kadarno P., Taha Z., "Vibration Analysis of Defected Ball Bearing using Finite Element Model Simulation", Proceedings of the 9th Asia Pasific Industrial Engineering & Management Systems Conference, (2008).**
3. **Michael S. Johnson Jr., P.E., "Vibration Tests for Bearing Wear", Ashrae Journal, Vol. 42(10), (2000).**
4. **Tadina M., Boltezar M., "Improved model of a ball bearing for the simulation of vibration signals due to faults during run-up", Journal of Sound and Vibration, Vol. 330 (17), pp. 4287-4301, (2011).**
5. **Kiral Z, Karagulle H., "Simulation and analysis of vibration signals generated by rolling element bearing with defects", Tribology International, Vol. 36(9), pp. 667–678, (2003).**
6. **Kiral Z, Karagulle H., "Vibration analysis of rolling element bearings with various defects under the action of an unbalanced force", Mechanical Systems and Signal Processing, Vol. 20(9), pp. 1967–1991, (2006).**
7. **Khanam S., Tandon N., Dutt J. K.," Multi-Event Excitation Force Model for Inner Race Defect in a Rolling Element Bearing", Journal of Tribology, Vol. 138, 011106-1, (2016).**
8. **Xu L., Yang Y. H., "Modeling a non-ideal rolling ball bearing joint with localized defects in planar multibody systems", Multibody Syst Dyn, Vol. 35, pp.409–426, (2015).**
9. **Khanam S., Dutt J. K., Tandon N.," Impact Force Based Model for Bearing Local Fault Identification", Journal of Vibration and Acoustics, Vol. 137, 051002-1, (2015).**

10. **Nabhan A, Nouby M., Sami A. M., Mousa M. O.," Vibration analysis of deep groove ball**
bearing with outer race defect using ABAQUS", Journal of Low Frequency Noise, Vibration and Active Control, Vol. 35(4), pp. 312–325, (2016).
11. **Nabhan A, Nouby M., Sami A. M., Mousa M. O.," Multiple Defects Detection in Outer Race of Gearbox Ball Bearing Using Time Domain Statistical Parameters", International Journal of Vehicle Structures & Systems, Vol. 8(3), pp. 167-174, (2016).**
12. **Khanama S., Tandona .N, Dutt J. K., "Fault size estimation in the outer race of ball bearing using discrete wavelet transform of the vibration signal", Procedia Technology, Vol. 14, pp. 12-19, (2014).**
13. **Zhang Y., Wang X., Yan X.," Dynamic Behaviors of the Elastohydrodynamic Lubricated Contact for Rolling Bearings", Journal of Tribology, Vol. 135 / 021501, (2013).**
14. **Zhu C., Gao L.," Quantitative Fault Analysis of Bearings Based on ADAMS", 3rd International Conference on Vehicle, Mechanical and Electrical Engineering, (2016).**
15. **Mishra C., Samantaray A. K., Chakraborty G.," Ball bearing defect models: A study of simulated and experimental fault signatures", Journal of Sound and Vibration, Vol. 400, pp. 86–112, (2017).**
16. **Choe B. S., Lee J. K., Jeon D., Lee Y.," Numerical Study of Cage Dynamics Focused on Hydrodynamic Effects of Guidance Land Clearances for Different Ball-Pocket Clearances in Cryogenic Environments", Journal of Engineering for Gas Turbines and Power, Vol. 140(4), 042502-1, (2018).**
17. **Kong F., Huang W, Jiang Y., Wang W., Zhao X., "Research on effect of damping variation on vibration response of defective bearings", Advances in Mechanical Engineering, Vol. 11(3), pp. 1–12, (2019).**
18. **Song M., Xiao S., Huang L., Li W.," Dynamic analysis of localized defects in rolling bearing systems", Vibroengineering Procedia., Vol. 14, pp. 34-39, (2017).**
19. **Gupta A., Agarwal R., Temani R., R. K. G., "Detection of Severity of Bearing Cage fault of Induction Motor with Externally Induced Vibration", International Journal of Advanced Research in Electrical, Electronics and Instrumentation Engineering, Vol. 3(4), (2014).**
20. **Kong F., Huang W., Jiang Y., Wang W., Zhao X.," A Vibration Model of Ball Bearings with a Localized Defect Based on the Hertzian Contact Stress Distribution", Shock and Vibration, , Article ID 5424875, (2018).**
21. **Dipen S., Shah, Patel V. N., "A Dynamic Model for Vibration Studies of Dry and Lubricated Deep Groove Ball Bearings Considering Local Defects on Races", Measurement, Vol. 137, pp. 535-555, (2019).**
22. **Sassi S., Badri B., Thomas M.," A Numerical Model to Predict Damaged Bearing Vibrations", Journal of Vibration and Control, Vol. 13(11), pp. 1603-1628, (2007).**